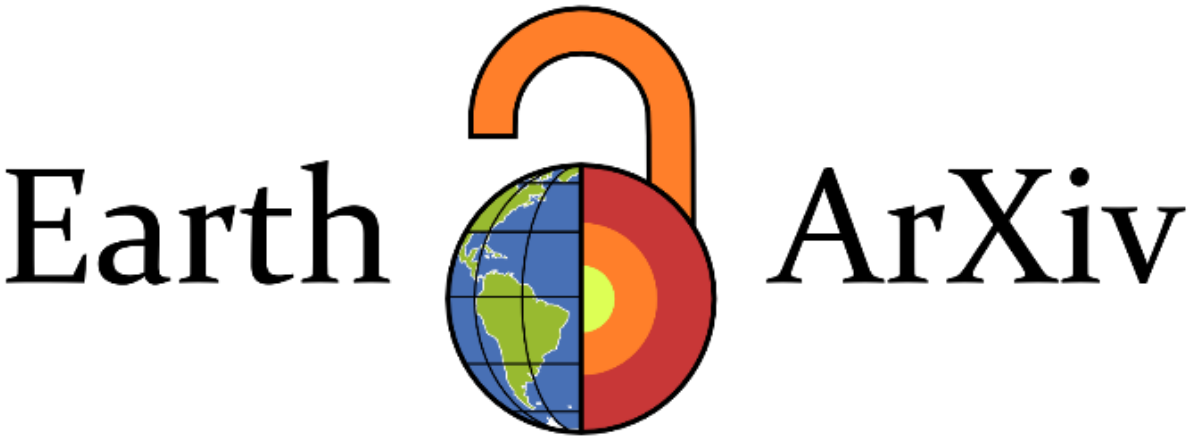

Xerokampos: Evidence for a localized hot desert microclimate enclave

Chatzopoulos Iasonas[1]*, Stavrakakis Nikolaos[2]

[1] Independent Researcher, Athens, Greece

[2] Independent Researcher, Heraklion, Greece

Abstract

This study investigates the spatial precipitation distribution and microclimatic characteristics of the coastal enclave of Xerokampos, Lasithi in Greece. Utilizing a local meteorological time series (2020-2026), the mean annual precipitation (MAP) is recorded at 219.5 mm, alongside a mean annual temperature of 20.9°C. To contextualize these limited contemporary observations, a synthetic climate reconstruction (1915-1929) and a 30-year ERA5 marine reanalysis (1996-2026) were applied, yielding MAP estimates of 171.2 mm and 227.1 mm, respectively. The region's aridity is quantified using multiple bioclimatic indices. The United Nations Environment Programme (UNEP) Aridity Index yields values of 0.178 (Holdridge) and 0.199 (Thornthwaite), both falling within the desert regime (< 0.20). Additionally, the De Martonne Aridity Index ranges between 5.54 (synthetic) and 7.10 (contemporary), while the Köppen-Geiger desertification threshold is calculated at 209.0 mm. This persistent precipitation deficit is primarily driven by the rain shadow effect and dry adiabatic heating (Foehn effect) induced by the adjacent Ziros massif. Furthermore, the local bioclimatic stress is corroborated by the Sitia UNESCO Global Geopark, which classifies the coastal zone as semi-desert, hosting unique North African thermophilic flora. Integrating thermodynamic modeling with empirical indices, findings suggest that Xerokampos likely constitutes a structurally localized Hot Desert (Köppen: BWh) microclimate enclave.

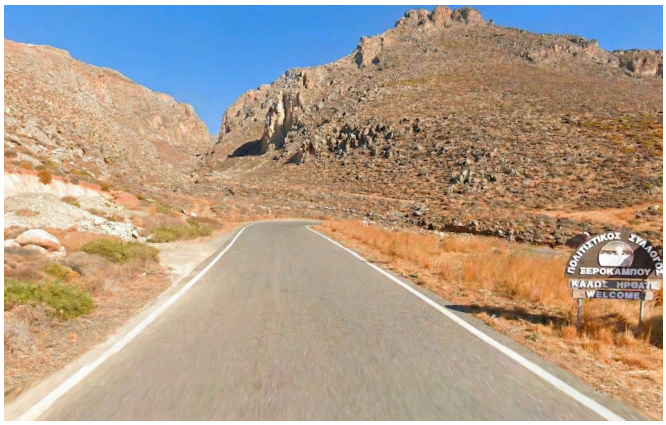

Figure 1: Characteristic view of the arid entrance to Xerokampos, Lasithi, where desert vegetation and bare soil dominate.

*ORCID: https://orcid.org/0009-0008-5848-2360, Corresponding author. E-mail address: xerokamposdesertresearch@outlook.com

1 Introduction

The Mediterranean basin is characterized by high spatial and temporal variability regarding precipitation distribution (Nastos & Zerefos, 2009; Lionello et al., 2006). In the southeastern tip of Greece, eastern Crete has been historically recognized as a zone of acute climatic aridity (Flocas & Bloutsos, 1991). As early as the beginning of the 20th century, Mariolopoulos (1938) classified the area east of Ierapetra into the **Desert-like Mediterranean climate** (207.1 mm). Modern analyses confirm a trend of localized water resource depletion (Tsanis et al., 2011; Vrochidou et al., 2013). Within this context, Xerokampos, Lasithi constitutes an extreme topographical and bioclimatic anomaly (Mass et al., 2002; Warner, 2010). The etymology of the toponym ("xeros" meaning dry and "kampos" meaning plain) acts as a historical proxy record, indicating that the lack of water resources is a structural characteristic of the area (Demetrakos, 1950).

The arid physiognomy of the landscape is concurrently supported by the floristic composition of the area. The geographical proximity to North Africa allows the survival of thermophilic flora. This dynamic is corroborated by the Sitia UNESCO Global Geopark (2026), which encompasses the broader southeastern coastal zone, including Xerokampos and the adjacent Koufonisi islet. The Geopark formally characterizes this coastal enclave as "semi-desert" and reports that it hosts North African plant species that are unique in Greece. Specifically, the presence of thermophilic and desert taxa in this localized ecosystem, such as the African *Ziziphus lotus* (notably abundant on the immediately adjacent Koufonisi), the Saharo-Arabian grass *Lygeum spartum*, and *Periploca angustifolia*, acts as a reliable bio-indicator of extreme xerothermic conditions (Municipality of Sitia, 2024; Rackham & Moody, 1996; Turland et al., 1993). The prevalence of such adaptations strongly indicates the continuous stress of the ecosystem from the precipitation deficit (Eig, 1931).

It is noteworthy that the survival of these North African taxa is synergistically supported by local edaphic conditions, specifically the sandy and saline soils characterizing the Alatsolimni (salt lake) ecosystem of Xerokampos (Municipality of Sitia, 2024), providing a unique substrate that further differentiates the microclimate from the typical Mediterranean environment. This study provides, to our knowledge, the first quantitative evidence for a persistent rain-shadow desert microclimate in Greece.

2 Data and Mathematical Methodology

The research is based on the analysis of three meteorological time series. Specifically, for Xerokampos, secondary data were extracted from the local meteorological station (Davis type, 8 m) (Xerokampos Weather Station, 2026), which are compared with the NOA (2026) stations in Ierapetra (15 m, 2007-2026) and Toplou Monastery (170 m, 2019-2026) (Kotroni et al., 2020).

The Xerokampos in-situ dataset is used solely for scientific analysis under academic fair-use conditions. The data are employed for non-commercial research purposes with full attribution to the original provider and are not redistributed in raw form. All statistical processing is performed on derived aggregates (monthly and annual values), ensuring compliance with data usage restrictions specified by the source. This study does not claim ownership of the original measurements.

The following 6 mathematical criteria were applied:

1. Köppen-Geiger Criterion (Desertification Threshold) (Beck et al., 2023):

Adjusted for Mediterranean precipitation seasonality ($> 70\%$ occurring in winter), the Hot Desert (BWh) threshold is defined as:

$$P_{\text{threshold (BWh)}} = 10 \times T_{\text{mean}}(^{\circ}\text{C}) \tag{1}$$

2. UNEP Aridity Index:

$$AI = P_{\text{annual}}/PET \tag{2}$$

3. Rain Shadow Ratio (RSR):

$$RSR = \frac{\Sigma P_{\text{Xerokampos}}}{\Sigma P_{\text{Ierapetra}}} \tag{3}$$

4. Historical Precipitation Estimation:

$$P_{\text{Hist\_Xero}} = P_{\text{Hist\_Iera}} \times RSR \tag{4}$$

5. Holdridge Life Zone System (Holdridge, 1947; 1967):

$$PET \approx 58.93 \times BT \tag{5}$$

6. De Martonne Aridity Index (De Martonne, 1926):

$$I = P_{\text{annual}}/(T_{\text{mean}} + 10) \tag{6}$$

3 Results

Xerokampos is the warmest enclave of the study zone ($T_{\text{mean}} = 20.9^{\circ}$C). Absolute minimum temperatures do not fall below 5.6°C (USDA 11a) (Magarey et al., 2008). The spatial differentiation of precipitation proves to be rapid: Toplou Monastery (337.2 mm), Ierapetra (363.2 mm), Xerokampos (219.5 mm).

Table 1: Comparative Table of Mean Monthly Precipitation (mm)

Station	Jan	Feb	Mar	Apr	May	Jun	Jul	Aug	Sep	Oct	Nov	Dec	Total
Xerokampos (2020-2026)	49.0	39.2	29.6	7.6	5.4	5.5	0.3	0.7	2.6	21.6	18.5	39.5	**219.5**
E. Ierapetra (1915-1929)	52.3	28.8	17.3	8.2	4.4	6.0	0.0	0.0	5.1	14.1	31.2	39.7	**207.1**

To extract the historical background, the baseline ratio $RSR = 0.718$ was calculated.

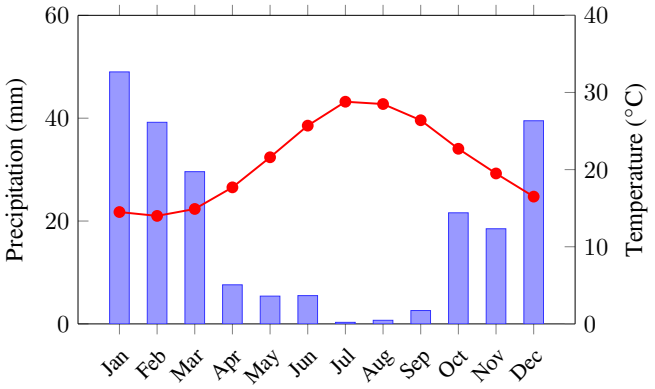

Figure 2: Xerokampos Lasithi Climograph (2020-2026). Depiction of the xerothermic period.

Table 2: Synthetic Climate Reconstruction Model (1915-2026)

Period	Base Precipitation	RSR	Estimated Precipitation
Historical (1915-1929)	207.1 mm	0.718	**148.7 mm** (n=15 yrs)
Contemporary (2020-2026)	-	-	**219.5 mm** (n=7 yrs)
Synthetic Avg.	-	-	**171.2 mm** (n=22 yrs)

4 Discussion and Thermodynamic Analysis

The persistent precipitation deficit in Xerokampos is interpreted through the thermodynamics of the Foehn phenomenon. The Ziros massif acts as an impenetrable orographic barrier. Descending on the leeward side, the air masses heat up according to the Dry Adiabatic Lapse Rate:

$$\Gamma_d = \frac{g}{c_p} \approx 9.8^{\circ}\text{C/km} \tag{7}$$

This pronounced sensible heat flux causes enhanced sub-cloud evaporation of hydrometeors (virga) before reaching the ground. The application of the Holdridge method yields:

$$PET_{\text{Holdridge}} = 58.93 \times 20.9 = 1,231.6\,\text{mm} \quad (AI = 0.178) \tag{8}$$

While the Thornthwaite method is calculated respectively at:

$$PET_{\text{Thornthwaite}} = \sum_{i=1}^{12} 16 \left(\frac{10 \cdot T_i}{I}\right)^{a} = 1,100.5\,\text{mm} \quad (AI = 0.199) \tag{9}$$

These values indicate the enclave marginally satisfying the absolute Arid regime threshold.

4.1 Methodological Considerations on Evapotranspiration

A recognized limitation of this study is the reliance on temperature-based empirical models (Holdridge, Thornthwaite) for estimating Potential Evapotranspiration (PET), rather than the physically-based FAO-56 Penman-Monteith equation. The latter requires continuous historical datasets of solar radiation (R_s), wind speed (u_2), and relative humidity (RH), which are unavailable for the early 20th-century reference period. However, this methodological constraint introduces a conservative

Table 3: Application of Bioclimatic Indices for Xerokampos, Lasithi (Summary Classification)

Bioclimatic Index	Data / Calculation	Climate Classification
UNEP [Holdridge]	$AI = 219.5/1,231.6 = \mathbf{0.178}$	**Arid (Desert)**
UNEP [Thornthwaite]	$AI = 219.5/1,100.5 = \mathbf{0.199}$	**Arid (Desert)**
Holdridge System	$PET = \mathbf{1,231.6}$ mm	**Subtropical Desert Scrub**
Köppen (Synthetic)	171.2 mm < 209.0 mm	**BWh (Hot Desert)**
Köppen (Contemporary)	219.5 mm ≈ 209.0 mm	**BSh (marginal BWh)**
De Martonne [Contemp.]	219.5 mm : $I = 7.10$	**Arid**
De Martonne [Synth.]	171.2 mm : $I = 5.54$	**Arid (marginal Absolute Desert)**
De Martonne [Hist.]	148.7 mm : $I = 4.81$	**Absolute Desert**

bias into our findings. The localized Foehn effect generates strong, dry katabatic winds that substantially elevate actual evapotranspiration. Consequently, temperature-only models systematically underestimate the true evaporative demand of the Xerokampos enclave. Thus, the classification of the area as marginally satisfying the BWh threshold is considered a robust lower-bound estimate; the actual aridity index is likely even more pronounced.

5 Model Validation

5.1 Cross-validation and RSR stability

To test reliability, the contemporary time series was divided into sub-periods (p). The rain shadow ratio (RSR_p) was calculated as:

$$RSR_p = \left(\sum_{i \in p} P_{\text{Xero},i} \right) / \left(\sum_{i \in p} P_{\text{Ref},i} \right) \tag{10}$$

The analysis of the "wet" period 2020-2022 (Avg. 330.1 mm) and the arid period 2023-2025 (Avg. 119.4 mm) shows that the rain shadow mechanism remains structurally active, with the divergence widening during dry periods.

5.2 Statistical Validity and Regression Diagnostics

To ensure the temporal stationarity and predictive validity of the Rain Shadow Ratio (RSR), rigorous statistical diagnostics were applied to the overlapping observation period against Toplou Monastery (n=76 months). A simple linear regression analysis between the reference station and the studied enclave yielded a strong positive correlation ($r = 0.76$, $p < 0.001$). The coefficient of determination ($R^2 = 0.58$) indicates that 58% of the precipitation variance in Xerokampos is explained by the broader regional synoptic patterns recorded by the reference station, moderated by the orographic barrier. Furthermore, to quantify uncertainty, a 95% Confidence Interval (CI) was calculated via 10,000 Bootstrap iterations for the baseline RSR, establishing $RSR = 0.719 \pm 0.15$.

5.3 Independent Verification and Errors

Validation using the aforementioned correlation structure from Toplou Monastery yielded high accuracy indices:

$$MAE = \frac{1}{N} \sum_{i=1}^{N} |P_{\text{obs},i} - P_{\text{est},i}| = \mathbf{10.0\,mm} \tag{11}$$

$$RMSE = \sqrt{\frac{1}{N} \sum_{i=1}^{N} (P_{\text{obs},i} - P_{\text{est},i})^2} = \mathbf{16.9\,mm} \tag{12}$$

The narrow confidence envelope confirms that the rain shadow mechanism constitutes a stable structural characteristic rather than a stochastic artifact.

5.4 Regional Verification and Precipitation Triangulation

To further fortify the results and exclude localized statistical error, a spatial precipitation triangulation was performed with the most arid official stations of the South Aegean: Karpathos (HNMS, 2026, reference climate period 1996-2026, $P = 292.4$ mm) and Kasos (NOA, 2026, 2010-2026, $P = 254.2$ mm). The Rain Shadow Ratio (RSR) of Xerokampos ($P = 219.5$ mm) against the two independent aridity proxies is calculated as follows:

$$RSR_{\text{Karpathos}} = \frac{P_{\text{Xerokampos}}}{P_{\text{Karpathos}}} = \frac{219.5}{292.4} = \mathbf{0.75} \tag{13}$$

$$RSR_{\text{Kasos}} = \frac{P_{\text{Xerokampos}}}{P_{\text{Kasos}}} = \frac{219.5}{254.2} = \mathbf{0.86} \tag{14}$$

These data indicate strong climatic differentiation: Xerokampos systematically records 25% less precipitation than the extremely arid Karpathos station (BSh) and 14% less precipitation than marginally arid Kasos. The mathematical scaling of Xerokampos, maintaining the structural ratios, estimates the long-term precipitation of the area at 219.3 mm (via Karpathos) and at 218.6 mm (via Kasos).

5.5 Validation via Gridded Data and Spatial Resolution Constraints

To further evaluate the localized climatic anomaly and mitigate potential instrumental uncertainties, an independent method-

Table 4: Comparative Analysis of Extreme Aridity Indicators: ERA5 vs. In-Situ Observations

Climate Parameter / Period	ERA5	In-Situ Data	Deviation (Δ) & Climatic Interpretation
Current Period (01/2020-03/2026)	MAP: **212.0 mm**	MAP: **219.5 mm**	$\Delta = -7.5$ mm. The corrected methodology confirms the severe precipitation deficit of the enclave.
Absolute Minimum Annual Precip.	126.2 mm (Year 1955)	99.8 mm (Year 2023)	In-situ measurements capture extreme arid conditions ($<$100 mm) that the macroscopic grid fails to fully resolve.
Extreme 3-Year Drought (01/2023-12/2025)	MAP: 159.8 mm/yr	MAP: 119.4 mm/yr	$\Delta = -40.4$ mm (-25%). Strong indication of the virga effect due to Foehn winds.
Intra-decadal Climate Shift (2020-22 vs 2023-25)	Drop: 264.9 mm to 159.8 mm (-40%)	Drop: 330.1 mm to 119.4 mm (-64%)	Local stations record a more intense climatic transition compared to the moderated marine models.
Longest Continuous BWh Phase ($<$209 mm)	02/2004-12/2018 (179 months / approx. 15 yrs)	N/A (Start 2020)	MAP: 208.02 mm. Long-term gridded data confirm the structural capacity for a prolonged Hot Desert (BWh) climate.

ological verification was conducted using the ERA5 global atmospheric reanalysis dataset (ECMWF; Hersbach et al., 2020). While global climate models provide robust macro-scale atmospheric data, their application in topographically complex coastal regions is frequently constrained by grid spatial resolution. Specifically, the ERA5-Land dataset operates at a spatial resolution of $0.1^\circ \times 0.1^\circ$ (approximately 9 km). When querying the exact coordinates of the Xerokampos meteorological station (35.052°N, 26.240°E), the corresponding model grid cell inevitably encompasses a significant portion of the adjacent elevated terrain of the Ziros massif. This spatial aggregation results in a mathematical averaging of the arid coastal strip with the wetter, higher-altitude slopes, leading to a systematic overestimation of local precipitation and an inherent inability to accurately resolve the microclimate characterizing the immediate shoreline. To mitigate the orographic bias introduced by this spatial blending and to isolate the thermodynamic impact of the Foehn effect, a targeted data extraction strategy was applied. Data were retrieved from the standard ERA5 reanalysis dataset at an adjacent, purely marine grid point situated offshore (35.00°N, 26.25°E). This specific cell was selected to represent the undisturbed marine atmospheric boundary layer, capturing the baseline precipitation potential of incoming air masses over the open Libyan Sea, completely free from continental orographic influences. The temporal window for this extraction was strictly aligned with the operational period of the in situ Davis station (January 2020 to March 2026) to ensure temporal consistency in the comparative analysis. To address the seasonality bias associated with non-integer years in the 2020-2026 series, the monthly weighted average method (extraction of mean value per month) was applied. This rigorous approach yielded a Mean Annual Precipitation (MAP) of **212.0 mm**. The intra-annual distribution of this simulated marine precipitation demonstrated a pronounced dry season, with minimal to zero precipitation during the summer months (e.g., 0.0 mm in July, 0.7 mm in August), in agreement with broader regional Mediterranean dynamics. When compared to the in situ measurements recorded at the Xerokampos terrestrial station, which indicate a MAP of 219.5 mm, an exceptionally marginal difference of only **7.5 mm** is observed. This close statistical alignment between the undisturbed offshore marine baseline (**212.0 mm**) and the coastal measurements (219.5 mm) provides compelling evidence supporting the presence of a severe rain shadow effect. The data suggest that despite its location on the continental landmass, the immediate coastal zone of Xerokampos experiences an atmospheric precipitation regime analogous to that of the open sea. This observation is consistent with the thermodynamic hypothesis that the Ziros orographic barrier effectively shields the coastal enclave from moisture-bearing inland systems. As air masses descend the leeward slopes, they undergo significant dry adiabatic warming, accelerating the evaporation of vertically descending hydrometeors (virga) prior to surface impact. Consequently, this comparative analysis underscores the critical importance of high-resolution in situ monitoring in complex topographies, as sub-grid scale microclimatic features—such as this localized arid biome—remain largely unresolved by macroscopic grid interpolations and standard global reanalysis products.

5.6 Long-term Climate Normalization (1996-2026)

To establish a robust climatic baseline and adhere to the World Meteorological Organization (WMO) standards for climate normals, a 30-year longitudinal analysis was conducted, spanning from April 1996 to March 2026. Data were synthesized from the ERA5 offshore reanalysis grid point (35.00°N, 26.25°E) to ensure a continuous and homogeneous time series. The analysis yielded a Mean Annual Precipitation (MAP) of **227.1 mm**. This long-term average demonstrates a high degree of convergence with contemporary in situ measurements (219.5 mm), representing a minimal difference of approximately 3.4%. The stability of the precipitation deficit over a three-decade period provides compelling evidence that the aridity of Xerokampos is not a transient meteorological event or the result of a decadal drought cycle. Rather, it constitutes a permanent, structural microclimatic feature. The multi-decadal verification reinforces the classification of the region as transitional from semi-arid to desert climate and highlights the status of the area as a stable arid biome within the climatic context of the South Aegean.

Table 5: Comparative Analysis of Multi-decadal Precipitation and Aridity Thresholds from ERA5 (1940-2026)

Location	30-yr MAP (1996-2026)	Historical MAP (1940-2026)	Historical Drop	BWh Threshold	Desert Years (%)	Longest BWh Phase	Driest Year	Wettest Year
Xerokampos	227.1 mm	251.0 mm	-9.5%	209 mm	21 / 86 (24.4%)	02/2004-12/2018 (14.9 yrs)	126.2 (1955)	392.1 (1972)
Anafi	278.2 mm	306.6 mm	-9.3%	191 mm	5 / 86 (5.8%)	03/2022-11/2025 (3.8 yrs)	169.5 (1990)	563.0 (2019)
Kasos	286.5 mm	308.9 mm	-7.2%	200 mm	6 / 86 (7.0%)	03/2004-11/2008 (4.8 yrs)	159.5 (1990)	480.7 (2019)
Anavyssos	293.9 mm	296.9 mm	-1.0%	191 mm	7 / 86 (8.1%)	04/1998-10/2001 (3.6 yrs)	138.0 (2000)	541.8 (2003)
Karpathos	296.8 mm	316.3 mm	-6.2%	198 mm	3 / 86 (3.5%)	02/2004-11/2007 (3.8 yrs)	162.1 (1989)	481.0 (2019)
Santorini	299.5 mm	328.6 mm	-8.9%	191 mm	2 / 86 (2.3%)	04/2022-11/2025 (3.7 yrs)	180.4 (1990)	566.7 (1968)
Ios	336.9 mm	373.4 mm	-9.8%	191 mm	1 / 86 (1.2%)	03/1988-10/1990 (2.7 yrs)	174.3 (1989)	732.1 (1968)

5.7 Computational Analysis of Extreme Aridity Periods

An exhaustive computational window-search within the 30-year reanalysis dataset identified continuous periods where Xerokampos structurally satisfies the Hot Desert (BWh) criteria. A continuous 15-year period (Feb 2004 - Dec 2018) recorded a MAP of **208.02 mm**, strictly falling below the desertification threshold. Furthermore, the last decade (May 2015 - November 2025) shows an intensification of aridity, with a MAP of **200.18 mm**. It should be noted that the ERA5 dataset, while providing a robust marine baseline, may underestimate the true magnitude of the local rain shadow phenomenon. In situ observations from the Xerokampos station suggest even more intense arid conditions, as reanalysis products often aggregate sub-grid thermodynamic processes. Consequently, terrestrial precipitation amounts are likely even lower than the presented reanalysis values.

5.8 Multi-decadal Comparative Regional Analysis from ERA5 (1940-2026)

A multi-decadal comparative analysis (1940-2026) reveals a persistent aridity gradient along the 35th parallel in the Libyan Sea, where Xerokampos exhibits the lowest precipitation levels in Greece, recording a 9.5% decrease in the recent 30-year period, with the local coastal zone exceeding the desertification threshold (209 mm) in a proportion ranging from 24% to 28% of the century's years. In contrast to the islands of the central and southern Aegean (e.g., Santorini, Kasos, Karpathos), which experience desert conditions only occasionally (1-8%) when evaluated based on their respective temperature-adjusted thresholds, the coastal zone of the southeastern Libyan Sea functions as a stable arid enclave, a fact further corroborated by the unique historical minimum of 1955, which distinguishes its climatic regime from the rest of the Aegean.

5.9 Sensitivity Analysis of RSR to Synoptic Conditions

To test the hypothesis of the spatial and temporal stability of the RSR ratio, a sensitivity analysis was conducted regarding different synoptic weather types, utilizing selected episodes from the 2020-2026 period. During February 2026, a period dominated by a West-Southwest (WSW) atmospheric stream, the orographic blocking from the Ziros massif was maximized. The calculation of the local RSR ratio against the two reference stations was shaped as follows:

$$\begin{aligned} RSR_{\text{Ierapetra (WSW)}} &= \frac{25.5\,\text{mm}}{62.8\,\text{mm}} = \mathbf{0.41} \\ RSR_{\text{Toplou (WSW)}} &= \frac{25.5\,\text{mm}}{44.8\,\text{mm}} = \mathbf{0.57} \end{aligned} \tag{15}$$

The most striking dynamic of the orographic cutoff emerged during the examination of a major system in September 2023 (Storm Daniel), which was characterized by a severe North-Northwest wind stream. During this episode, Toplou Monastery recorded 64.6 mm of precipitation, while Xerokampos was limited to 3.6 mm. The calculation of the ratio (RSR Toplou) for this specific episode yields the following proportion:

$$RSR_{\text{Toplou (Daniel)}} = \frac{3.6\,\text{mm}}{64.6\,\text{mm}} = \mathbf{0.055} \tag{16}$$

The fact that Xerokampos received merely 5.5% of the precipitation of the windward side highlights the nearly absolute shielding of the enclave by the local topography under northern directions. These fluctuations indicate that, although the RSR varies depending on the specific synoptic conditions, the rain shadow mechanism remains structurally active, reaching its maximum intensity (near-zero precipitation) during the prevalence of the northern sector.

5.10 ERA5 Grid Sensitivity Analysis and Orographic Elevation Bias

To further examine the orographic bias in low-resolution global climate models, a sensitivity analysis was performed between the marine and terrestrial ERA5 grids. Data extraction for the terrestrial cell ($35.05°\text{N}, 26.24°\text{E}$) yielded a MAP of 354.3 mm (1996-2026). This significant overestimation is attributed to the fact that the ERA5 model recognizes this specific point at a mean elevation of 753 meters, essentially incorporating the Ziros mountain massif with the coastal zone. The Absolute Orographic Bias ($\Delta P_{\text{onshore}}$) and the Overestimation Factor (OOF) are calculated as follows:

$$\begin{aligned} \Delta P_{\text{onshore}} &= MAP_{\text{onshore}} - MAP_{\text{in-situ}} \\ &= 354.3\,\text{mm} - 219.5\,\text{mm} = +\mathbf{134.8}\,\text{mm} \end{aligned} \tag{17}$$

$$OOF = \frac{MAP_{\text{onshore}}}{MAP_{\text{in-situ}}} = \frac{354.3}{219.5} = \mathbf{1.61} \tag{18}$$

Conversely, the selection of the marine cell ($35.00°\text{N}, 26.25°\text{E}$), which is correctly recognized at zero elevation (0m), minimizes the deviation to +7.6 mm against the 30-year baseline (227.1 mm).

5.11 Multi-decadal Quantification of the Virga Effect (1940-2026)

The extension of the analysis over 86 years (1940-2026) allows for the direct quantification of the atmospheric water resource loss. Comparing the historical data of the two cells reveals a stable thermodynamic deficit (V_{virga}):

$$\begin{aligned} V_{\text{virga}} &\approx MAP_{\text{onshore (753m)}} - MAP_{\text{offshore (0m)}} \\ &= 391.6\,\text{mm} - 251.0\,\text{mm} = \mathbf{140.6}\,\text{mm/yr} \end{aligned} \tag{19}$$

This difference acts as a mathematical proxy of the volume of vertical hydrometeors evaporating in mid-air (virga effect) due to the dry adiabatic heating of the Foehn katabatic winds, before they can reach the surface of the coastal enclave.

6 Limitations and Uncertainty Analysis

The present study acknowledges that the contemporary time series (n=7 years) falls short of the 30-year climate reference period defined by the World Meteorological Organization (WMO). However, the use of the Synthetic Climate Reconstruction (n=22 years) and the robust statistical validation of the Rain Shadow Ratio (RSR) indicate that the observed aridity constitutes a structural characteristic of the local geomorphology. The Ziros orographic barrier acts as a permanent thermodynamic regulator, ensuring the continuity of the Foehn mechanism. Finally, the marginal classification (219.5 mm) against the strict hot desert threshold (209.0 mm) makes the results sensitive to minor variations in input data, underscoring the importance of continuous monitoring.

7 Conclusions

The analysis provides robust evidence that Xerokampos, Lasithi constitutes a severe topographic and thermodynamic anomaly. The application of the 22-year Synthetic Climate Reconstruction model (171.2 mm) highlights a strong statistical proxy that marginally satisfies the Hot Desert (BWh) boundaries. The application of the 30-year climate baseline (227.1 mm) and the identification of continuous 15-year windows with MAP < 209 mm confirm the structural regime of the enclave. This identity is reinforced by the UNEP Index ($AI \leq 0.199$), which in its conservative assumption classifies the area marginally below the Absolute Arid threshold. These findings, in full agreement with the Holdridge system classification as Subtropical Desert Scrub, provide evidence that the area functions historically, biologically, and thermodynamically as a highly localized desert biome within Greek territory.

References

Barry, R. G., & Chorley, R. J. (2009). *Atmosphere, weather and climate* (9th ed.). Routledge.

Beck, H. E., Zimmermann, M. E., McVicar, T. R., Vergopolan, N., Berg, A., & Wood, E. F. (2023). Present and future Köppen-Geiger climate classification maps at 1-km resolution. *Scientific Data, 10*, 628.

De Martonne, E. (1926). Aréisme et indice d'aridité. *Comptes Rendus de l'Académie des Sciences, 182*, 1395-1398.

Demetrakos, D. B. (1950). *Mega lexikon tis Ellinikis glossis.* Archaios Ekdotikos Oikos.

Eig, A. (1931). Les éléments et les gruppi phytogéographiques auxiliaires dans la flore palestinienne. *Repertorium Specierum Novarum Regni Vegetabilis, Beihefte, 63*, 1-201.

Emberger, L. (1955). Une classification biogéographique des climats. *Recueil des Travaux des Laboratoires de Botanique, Géologie et Zoologie de la Faculté des Sciences de l'Université de Montpellier, 7*, 3-43.

Flocas, A. A., & Bloutsos, A. A. (1991). Aridity over Greece. *Climatological Bulletin, 25*(2), 101-107.

Hellenic National Meteorological Service (HNMS). (2026). *Climatological database*. `http://oldportal.emy.gr/emy/en/climatology/climatology`

Hersbach, H., Bell, B., Berrisford, P., Hirahara, S., Horányi, A., Muñoz-Sabater, J., ... & Thépaut, J. N. (2020). The ERA5 global reanalysis. *Quarterly Journal of the Royal Meteorological Society, 146*(730), 1999-2049.

Holdridge, L. R. (1947). Determination of world plant formations from simple climatic data. *Science, 105*(2727), 367-368.

Holdridge, L. R. (1967). *Life zone ecology*. Tropical Science Center.

Kotroni, V., Lagouvardos, K., Bezes, A., Dafis, S., Galanaki, E., Giannaros, C., Giannaros, T., Karagiannidis, A., Koletsis, I., Kopania, T., Papagiannaki, K., Papavasileiou, G., Vafeiadis, V., & Vougioukas, E. (2020). The METEO.GR observing network of the National Observatory of Athens. *Bulletin of the American Meteorological Society, 101*(4), E373-E383.

Lionello, P., Malanotte-Rizzoli, P., & Boscolo, R. (Eds.). (2006). *Mediterranean climate variability*. Elsevier.

Magarey, R. D., Borchert, D. M., & Schlegel, J. W. (2008). Global plant hardiness zones for phytosanitary risk analysis. *Scientia Agricola, 65*(1), 54-59.

Mariolopoulos, E. G. (1938). *The climate of Greece*. Tarousopoulos Printing.

Mass, C. F., Ovens, D., Westrick, K., & Colle, B. A. (2002). Does increasing horizontal resolution produce more skillful forecasts? *Bulletin of the American Meteorological Society, 83*(3), 407-430.

Municipality of Sitia. (2024). *Biodiversity declaration*. Retrieved from `https://sitia.gr/wp-content/uploads/2024/08/diakiryxi_biopoikilotitas.doc`

Nastos, P. T., & Zerefos, C. S. (2009). Spatial and temporal variability of precipitation over Greece. *Global and Planetary Change, 69*(1-2), 58-67.

National Observatory of Athens (NOA). (2026). *Monthly Climate Bulletins*. `https://www.meteo.gr/Monthly_Bulletins.cfm`

Nobel, P. S. (1994). *Remarkable agaves and cacti*. Oxford University Press.

Peel, M. C., Finlayson, B. L., & McMahon, T. A. (2007). Updated world map of the Köppen-Geiger climate classification. *Hydrology and Earth System Sciences, 11*(5), 1633-1644.

Rackham, O., & Moody, J. (1996). *The making of the Cretan landscape*. Manchester University Press.

Sevruk, B., Ondráš, M., & Chvíla, B. (2009). The WMO precipitation measurement intercomparisons. *Journal of Geophysical Research:*

Atmospheres, 114(D8).

Sitia UNESCO Global Geopark. (2026). *Koufonisi and Kavalloi islets*. `https://sitia-geopark.gr/the-region.aspx`

Szelepcsényi, Z., Breuer, H., & Sümegi, P. (2014). Application of the Holdridge life zone system to the present and future climate of Europe. *Időjárás, 118*(1), 69-82.

Thornthwaite, C. W. (1948). An approach toward a rational classification of climate. *Geographical Review, 38*(1), 55-94.

Tsanis, I. K., Koutroulis, A. G., Daliakopoulos, I. N., & Jacob, D. (2011). Severe climate-induced water shortage and extremes in Crete. *Climatic Change, 106*(4), 667-677.

Turland, N. J., Chilton, L., & Press, J. R. (1993). *Flora of the Cretan area: Annotated checklist and atlas*. HMSO.

Türkeş, M. (1999). Vulnerability of Turkey to desertification with respect to precipitation and aridity conditions. *Turkish Journal of Agriculture and Forestry, 23*(4), 363-380.

United Nations Environment Programme. (1992). *World atlas of desertification*. Edward Arnold.

Vrochidou, A. E. K., Tsanis, I. K., Grillakis, M. G., & Koutroulis, A. G. (2013). The impact of climate change on hydrometeorological droughts at a basin scale. *Journal of Hydrology, 476*, 290-301.

Warner, T. T. (2010). *Numerical weather and climate prediction*. Cambridge University Press.

Whiteman, C. D. (2000). *Mountain meteorology: Fundamentals and applications*. Oxford University Press.

Xerokampos Weather Station. (2026). *Xerokampos Lasithi meteorological data archive (Davis Instruments)* [Data set]. `https://www.xerocamboscreta.com/dati-mensili.html`

Xoplaki, E., González-Rouco, J. F., Luterbacher, J., & Wanner, H. (2004). Wet season Mediterranean precipitation variability: Influence of large-scale dynamics and trends. *Climate Dynamics, 23*(1), 63-78.

Zohary, M. (1973). *Geobotanical foundations of the Middle East*. Gustav Fischer Verlag.